Biointerface Research in Applied Chemistry
Open-Access Journal (ISSN: 2069-5837)

Article
Volume 13, Issue 1, 2023, 56
https://doi.org/10.33263/BRIAC131.056

Removal of Phosphate from Synthetic Wastewater by Using Marsh Clam (*Polymesoda expansa*) Shell as an Adsorbent

Noorul Hudai Abdullah [1,*], Ong Jing Xian [2], Chiew Zhi Yi [2], Ng Shi Yuan [2], Mohamad Syahrul Syazwan Yaacob [3], Nur Atikah Abdul Salim [4], Noraziah Ahmad [5], Zainab Mat Lazim [4], Maria Nuid [6], Faizuan Abdullah [7]

1 Neo Environmental Technology, Centre for Diploma Studies, Universiti Tun Hussein Onn Malaysia, Pagoh Education Hub, 84600 Pagoh, Johor, Malaysia
2 Centre for Diploma Studies, Universiti Tun Hussein Onn Malaysia, Pagoh Education Hub, 84600 Pagoh, Johor, Malaysia
3 Faculty of Engineering Technology, Universiti Tun Hussein Onn Malaysia, Pagoh Education Hub, 84600, Johor, Malaysia
4 School of Civil Engineering, Faculty of Engineering, Universiti Teknologi Malaysia, 81310 UTM Johor, Malaysia
5 Faculty of Civil Engineering Technology, Universiti Malaysia Pahang, Lebuhraya Tun Razak, Kampung Melayu Gambang, 26300 Gambang, Pahang
6 Centre for Environmental Sustainability and Water Security, Research Institute for Sustainable Environment, Universiti Teknologi Malaysia, 81310 UTM Skudai, Johor Bahru, Malaysia
7 Department of Chemistry, Faculty of Science, Universiti Teknologi Malaysia, 81310 UTM Johor Bahru, Johor, Malaysia
* Correspondence: noorul@uthm.edu.my (N.H.A.);

Scopus Author ID 57217560465
Received: 18.11.2021; Accepted: 17.12.2021; Published: 30.01.2022

Abstract: Phosphate pollution is becoming a serious problem worldwide. It leads to increased algae growth, resulting in eutrophication, which affects the water bodies' quality, the lives of aquatic organisms, and the daily routines of humankind. Previous research has proven effective chemical precipitation for phosphate removal, but the cost is high and may generate waste material. Thus, this study proposed the marsh clam (*Polymesoda expansa*) shell as an absorbent due to its abundant availability, low cost, and high absorption capacity of phosphorus. This study was conducted to investigate the removal efficiency of phosphate using raw marsh clamshells. In this study, the concentration of aqueous solution using KH_2PO_4 was fixed to 10 mg/L of PO_4^{3-} as the initial concentration. The 2 g of mass absorbent (0.075mm, 0.15mm, 0.30 mm, 0.60 mm, 1.18 mm, 2.36 mm) mixed with 100mL of KH_2PO_4 solution in the conical flask in a certain time interval. The orbital shaker was used for mixing the KH_2PO_4 solution with the adsorbent. Moreover, HACH DR 6000 Spectrophotometer is then used to determine phosphate concentration for initial and final results. The results were verified using kinetic and isotherm models, where kinetic models used Pseudo First Order (PFO) and Pseudo Second Order (PSO). The isotherm model used the Freundlich and Langmuir models. The optimum performance of the batch experiment showed by the PSO model had the highest correlation coefficient (R_2 = 0.9965) and the lowest F_e value of 0.086. This study showed that marsh clamshells could remove PO_4^{3-} effectively for 1.18–2.36 mm size with the highest removal efficiency of 73%. The removal of phosphate from domestic wastewater can be an alternative wastewater treatment in tertiary treatment in the field of the wastewater treatment plant.

Keywords: Marsh clam shells; phosphate removal; adsorbent; *Polymesoda expansa*.

1. Introduction

Wastewater treatment is important to solving in Malaysia and among other developed countries. Wastewater could affect water quality and result in serious consequences for people if people do not manage the wastewater well [1]. Wastewater issues can lead to ecosystem loss, which becomes an economic opportunity and climate change causes wastewater that releases gases such as methane and nitrous oxide [2]. Since the main water supply for our country comes from surface water, issues on the quality of water should be addressed seriously [3].

Phosphate is commonly found in the organic waste in sewage that comes from agricultural fertilizers that help the plant growth and play an important role in restoring plant communities of heavy metals polluted soils [4]. For plant life, phosphate is also an essential element. However, the high phosphate concentration will disadvantage the environment due to the excess of phosphate. The excess of phosphorus will lead to eutrophication which means the gradual increase in the concentration of phosphorus, nitrogen, and other plant nutrients in an aging aquatic ecosystem such as a lake [5]. Recently, adsorption has become a technique used to remove the pollutant from the water by using materials such as crab shells [6], eggshell [7], duck eggshells [8], oyster shells [9], mussel shells [10,11]. So, this study removes phosphate from an aqueous solution [12].

This study used raw marsh clamshell (MCS) as an absorbent to adsorb phosphate in the wastewater. This is because the content of MCS is high in calcium oxide that can adsorb the phosphate component. Moreover, the MCS is a waste that is discarded in illegal places; due to hard to decompose naturally, it can cause serious pollution due to the exposure of wasted MCS [13].

This research was conducted to investigate the removal efficiency of phosphate using raw MCS, to compare the removal performance of phosphate under different types of adsorbents and different particle sizes. This study also analyses the adsorption model using kinetic and isotherms models based on the data of the batch experiment.

2. Materials and Methods

2.1. Adsorbent.

The adsorbent used in this research was the MCS collected from Kelantan, one of the states in Malaysia, and transported to the University of Tun Hussein Onn Malaysia. After that, the MCS was cleaned using tap water to remove the impurities and contaminants on the shells. The cleaned MCS were rinsed using distilled water and dried under sunlight and oven at 30°C. When the shells dry, they were crushed using mortar and pestle. The crushed shells were prepared in different sizes, which are 1.18–2.36 mm, 0.60–1.18 mm, 0.30–0.60 mm, 0.15–0.30 mm, and 0.075–0.15 mm through the sieving process. All the prepared adsorbents were sealed in a desiccator to ensure they did not affect the humidity [14]. The adsorbents were characterized for physicochemical analysis at the University Tun Hussein Onn Malaysia Laboratory.

2.2. Synthetic solution.

A 10 mg/L synthetic phosphorus solution was prepared by dissolving 0.1433 g of KH_2PO_4 in distilled water in a 1L volumetric flask [15]. The concentration of the phosphorus solution was measured using the Amino Acid Method according to the Standard Methods for

the Examination of Water and Wastewater [16]. The filter paper and the vacuum pump were used to filter the suspended adsorbent.

2.3. Analytical methods.

The orbital shaker was used to mix the KH_2PO_4 solution with the adsorbent. It was set at 170 rpm. The phosphate content, P, was measured using HACH DR 6000 UV-Vis Spectrophotometer and calculated using the amino acid method 490 for phosphate according to the Standard Methods for the Examination of Water and Wastewater was used for all parameters [17].

The unmodified surface morphology absorbent was characterized using Scanning Electron Microscope (SEM) (EM-30AX Plus; COXEM, Daejeon, Korea). The second-generation BRUKER D2 Phaser benchtop X-Ray Diffraction (XRD) was used to identify the mineral phases in the raw MCS. Fourier Transform Infrared (FTIR) Spectroscopy (Perkin Elmer Spectrum Two FTIR Spectrometer, United States America) was used to identify the raw MCS functional group. Energy dispersive X-Ray Fluorescence (EM-30AX Plus; COXEM, Daejeon, Korea) was used to analyze the chemical composition of raw MCS in percentage [18-20].

2.4. Batch experiment.

In this experiment, the concentration of the phosphate solution was fixed at 10 mg L^{-1} or 10 ppm. A total of 2 g absorbents were weighed using electronic balance per plastic bag and packed in 10 plastic bags.

Table 1. The time set for phosphate adsorption.

Flask No.	0	1	2	3	4	5	6	7	8	9	10
Adsorbent (g)	2										
Volume of KH_2PO_4 (mL)	100										
Time (min)	0	30	60	120	180	300	420	1440	2880	4320	5760
Day	Day1							Day 2	Day 3	Day 4	Day 5

For the adsorption test, 2 g of absorbent was added into 100 mL of KH_2PO_4 solution. All samples were placed on the orbital shaker to mix the phosphate solution at 170 rpm. All ten samples were syringed out at the set times of 30 min, 60 min, 120 min, 180 min, 300 min, 420 min, 1440 min, 2880 min, 4320 min, and 5760 min (the minutes were calculated from 0 min) for 5 days. Samples were vacuum filtered using filter papers and analyzed using the DR 6000 Spectrometer. All information is shown in Table 1. The results were analyzed using the Pseudo First Order (PFO) and Pseudo Second Order (PSO), Freundlich, and the Langmuir models [21].

3. Results and Discussion

Physicochemical characteristics of MCS, including EDXRF, SEM, and FTIR, were investigated. The kinetic and isotherm model was used to describe phosphate adsorption onto raw MCS.

3.1. Physicochemical characteristics of MCS.

As shown in Table 2, the major elements of MCS used in this study are Ca (27.96%), O (55.33%), and C (15.84%). Meanwhile, the minor elements are Na (0.56%), Al (0.08%), Fe (0.06%) and Sr (0.17%).

Table 2. Composition of the raw MCS (in weight%) by EDXRF

wt.%	Ca	O	C	Na	Al	Fe	Sr
Raw MCS	27.96	55.33	15.84	0.56	0.08	0.06	0.17

A similar percentage of waste shell composition such as shrimp shell, where the content of Ca (22.52%), O (35.80%), C (25.38%), supported with minor element N (2.94%) and P (13.36%) [22] have been analyzed. Figure 1 shows 1500, 6000, 10000 times of magnification of MCS surface by using SEM. Figure 1 (a), (b), and (c) shows that the raw MCS had an irregular, rough the porous surface structure. From Figure 1 (c), 10000 times of magnification displayed uniform porosity of MCS surface containing high Ca and O composition to adsorb phosphate in solution.

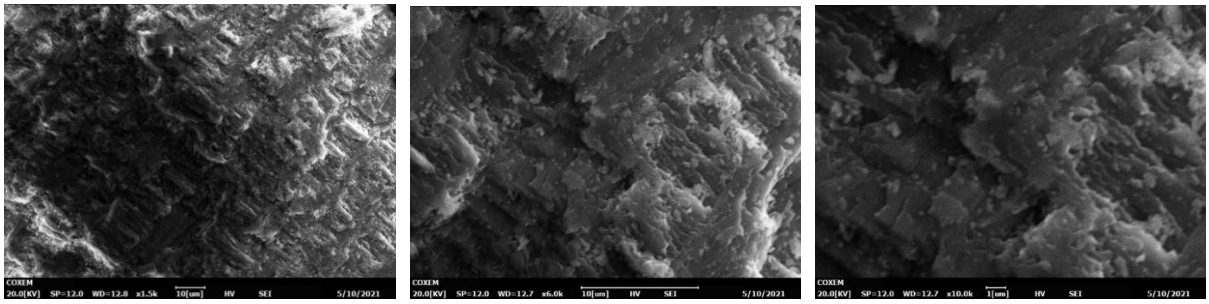

(a) (b) (c)

Figure 1. The SEM photomicrograph of MCS: (a) SEM images of 1500×, (b) 6000×, (c) 10000× magnification.

Table 3. FTIR spectral characteristics of raw MCS before and after adsorption.

No	Frequency spectrum (cm^{-1})			Detection of functional group	References
	Before adsorption	After adsorption	Differences		
1	1459.36	1455.63	3.73	Methylene C-H bend	[23]
2	1082.78	1082.89	0.11	P–O bending	[12]
3	857.45	856.92	0.53	C-O-O- stretch	[23]
4	712.68	712.77	0.09	Peroxides, Fe–O–H bending	[12]
5	699.82	699.93	0.11	C-Br stretching bands	[24]

The Fourier Transform Infrared (FTIR) was used to identify the chemical bonds in the raw MCS by producing an infrared absorption spectrum. It helps measure the infrared region of the electromagnetic radiation spectrum [25]. In this case, the raw MCS was used as an adsorbent to absorb the phosphate. Before the absorption process, the reading of the FTIR was 1459.36 cm^{-1}, 1082.78 cm^{-1}, 857.45 cm^{-1}, 712.68 cm^{-1}, and 699.82 $cm^{-1,}$ respectively. The results obtained after absorption were 1455.63 cm^{-1}, 1082.89 cm^{-1}, 856.92 cm^{-1},712.77 cm^{-1}, and 699.93 cm^{-1}. The FTIR results were plotted into a graph (Figure 2). Table 3 shows the functional groups found from the samples before adsorption and after absorption.

XRD is used to identify inorganic 'materials' phase purity and crystallinity [26]. The XRD plot (Figure 3) indicates the presence of aragonite and calcium carbonate. The red line represents aragonite, whereas the blue one represents calcium carbonate. [27] also reported that $CaCO_3$ has good absorption ability for PO_4^{3-} ion. High calcium content material may increase PO_4^{3-} absorption [28].

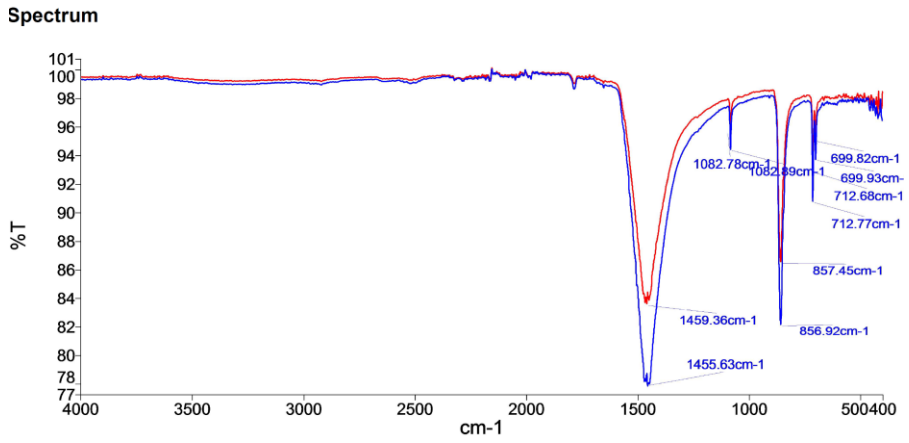

Figure 2. The FTIR spectra of raw MCS, the result before the absorption process represented by the red color line, and the blue color representative the result after absorption.

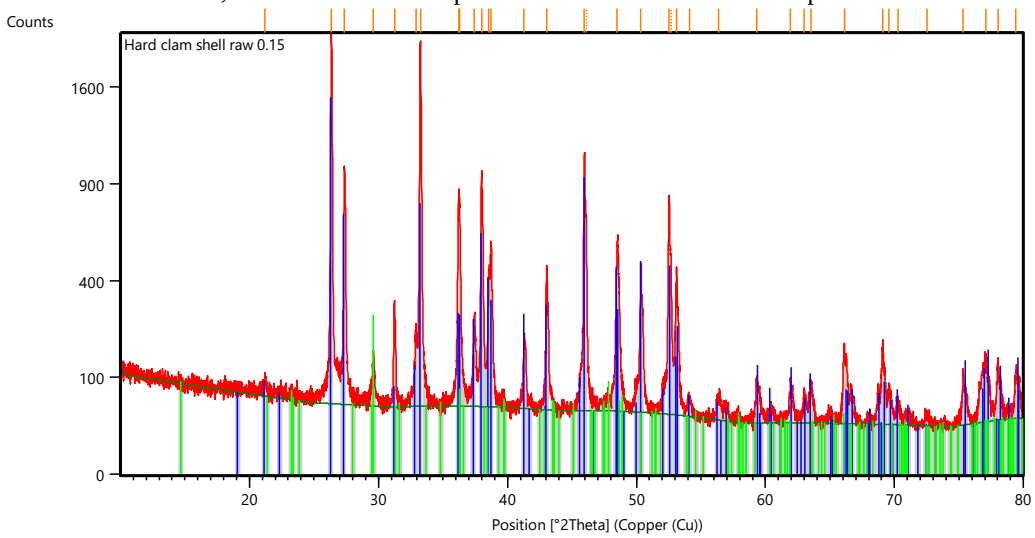

Figure 3. The XRD plot.

3.2. Effect of adsorption capacity, q (mg g^{-1}).

Adsorption capacity is when the adsorbent took up adsorbate per unit mass of the adsorbent [29]. 100 mL of aqueous solution mixed with 2g of MCS adsorbent were used to identify the equilibrium state of adsorption capacity. Figure 4 shows that the biggest size of the absorbent had the biggest adsorption capacity, where Figure 4 (a) indicates the highest of adsorption capacity at equilibrium state (0.368 mg g^{-1}) to recover phosphate in solution, reached at 5760 min for 1.18mm for particle size of MCS adsorbents. Although this particle size was taken for a long time to achieve an equilibrium state, it shows high removal efficiency at the end of the adsorption process. This adsorption capacity of the equilibrium state is important for the kinetic and isotherm model.

3.3. Effect of removal efficiency, E (%).

The removal efficiency, E (%) of phosphate from solution was studied for 5760 min, and it indicates the performance of 2g of adsorbent dose with 10 mg L^{-1} of concentration constant shown in Figure 5. It was found that the increase of time increases the removal efficiency. The highest removal efficiency (72.97%) was observed from the MCS size 1.18 mm and was followed by size 0.075 mm with 67.34% phosphate adsorbed. Figure 5 shows the lowest removal efficiency of phosphate for 0.6 mm particle size of raw MCS, given 18.42% adsorption. The result shows 1.18 mm of particle size of MCS adsorbent was performed in

removing the phosphate, and it indicates the porous surface of adsorbent saturated of all active sites [30].

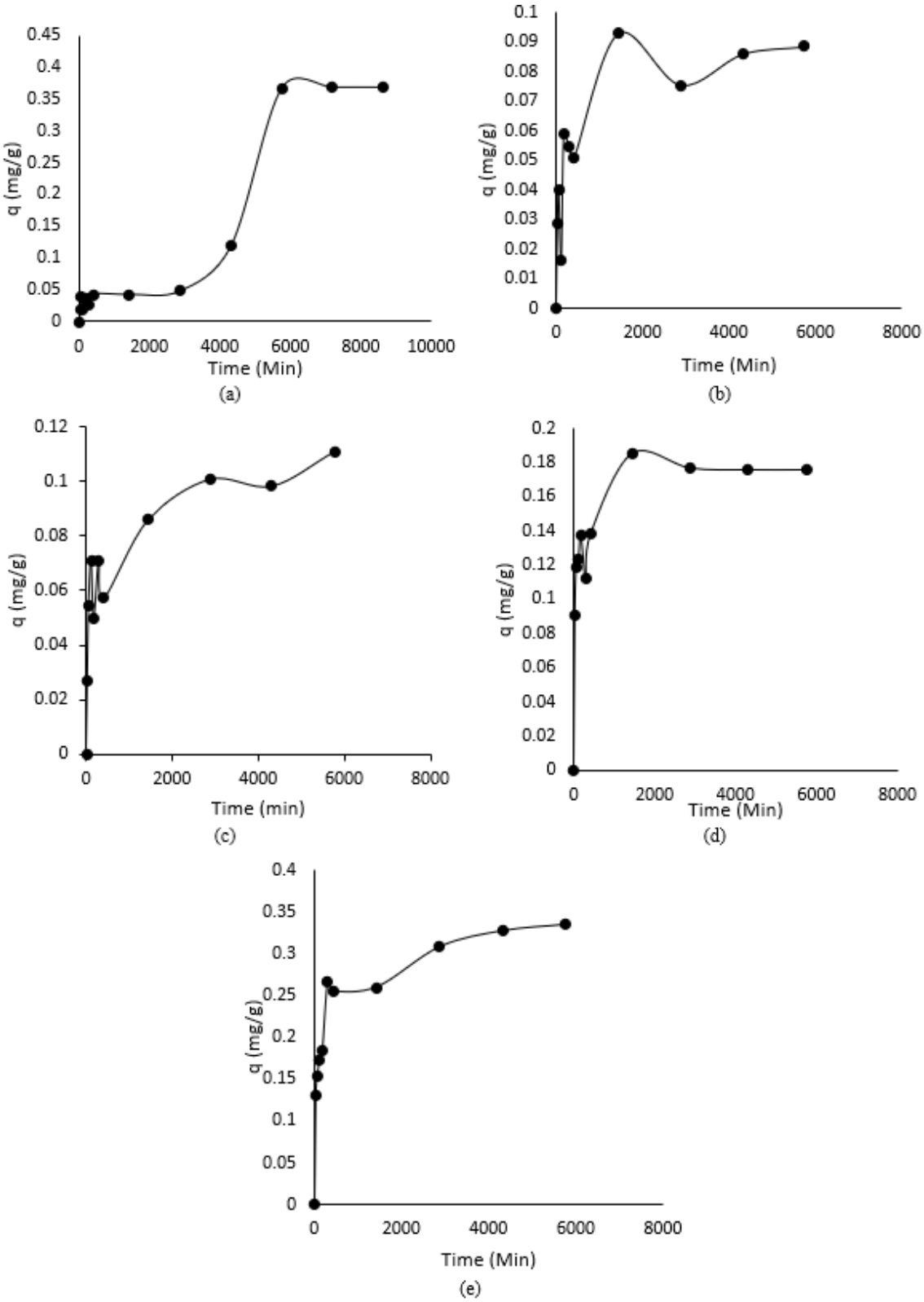

Figure 4. The adsorption capacity of MCS for (a) size 1.18 mm (b) size 0.60 mm (c) size 0.30 mm (d) size 0.15 mm (e) size 0.075 mm.

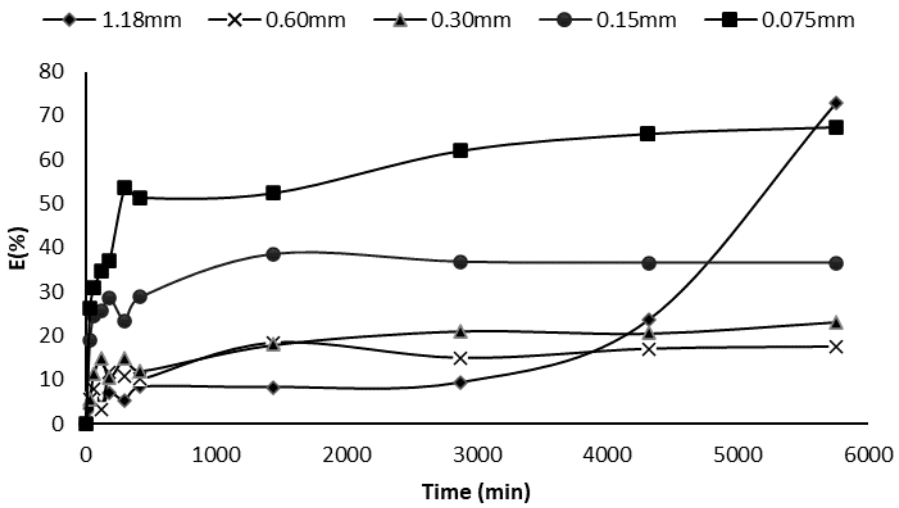

Figure 5. The removal efficiency with contact time for every particle size.

3.4. Pseudo-first-order (PFO) kinetic model.

Eq. 1 was used to plot the graph for PFO model as a linear plot.

$$\ln[q_e - q(t)] = \ln q_e - k_1 t_i \qquad \text{Eq. 1}$$

where q is equal to the amount of the absorbed solute, q_e is equal to the amount of absorbed solute at equilibrium, k_1 is PFO constant, and t is time. The term equilibrium means that when the solution achieves saturated concentration, the removal process of an adsorbent will not occur again [31].

From the general equation of a linear line is $y = mx + c$, where m represents gradient, c represents the intercept at y-axis [32]. Therefore, comparing the linear equation of PFO and the general equation of a linear line, thus the $\ln[q_e - q(t)]$ represent y, $\ln q_e$ represent c, $-k_1$ represent m, t_i represent x. Figure 6 shows the parameter of PFO for the adsorption.

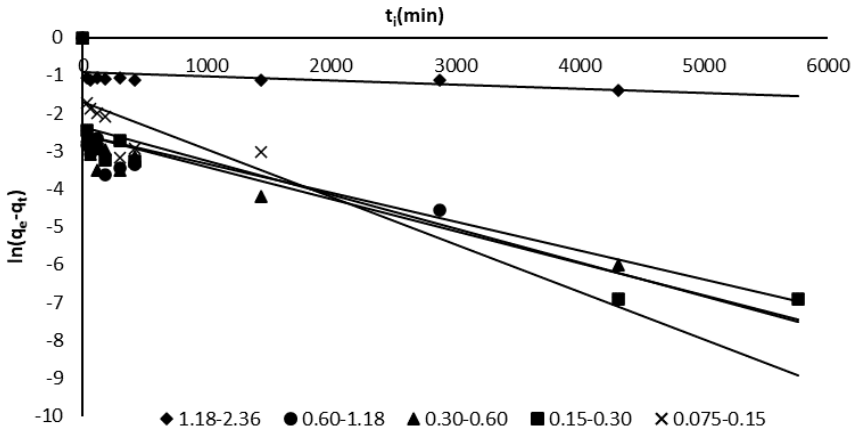

Figure 6. Linear line of plotting for PFO with different particle sizes.

Table 4. The kinetic parameter of the PFO model.

Sample	*Particle Size (mm)*	*q_e (theo) (mg g^{-1})*	*k_1 (min^{-1})*	*R^2*	*F_e*	*q_e (exp) (mg g^{-1})*
Synthetic solution	1.180–2.360	0.403	0.0001	0.199	0.318	0.368
	0.600–1.180	0.077	0.0008	0.031	0.116	0.086
	0.300–0.600	0.076	0.0008	0.577	0.178	0.101
	0.150–0.300	0.093	0.0009	0.800	0.530	0.177
	0.075-0.150	0.182	0.0013	0.337	0.660	0.309

Table 4 shows the parameters of q_e, k_1, R^2, and F_e. The value for parameter F_e can be obtained using Eq.2. The suitable model for the adsorption process will have the highest R^2 and lowest F_e [12].

$$F_e = \sqrt{\left(\frac{1}{n-p}\right)\sum_i^n \left(q_{t(exp)} - q_{t(theo)}\right)^2} \qquad \text{Eq. 2}$$

In Eq. 2, n represents the number of measurements, p represents the number of kinetic parameters, $q_{t(exp)}$ represents the experimental q value, and $q_{t(theo)}$ represents the theoretical q value (mg g^{-1}).

3.5 Pseudo-second order (PSO) model.

In order to plot the graph for the PSO model, Eq.3 was used as the linear equation,

$$\frac{t_i}{q_t} = \frac{1}{k_2 q_e^2} + \frac{t_i}{q_e} \qquad \text{Eq. 3}$$

where q_t is the amount of absorption at time t, qe is the amount of absorption at equilibrium, k_2 is the constant of PSO [33].

From the general equation of a linear line, $y = mx + c$, m represents the gradient, c represents the intercept at the y-axis [32]. Therefore, for PFO, $\frac{t_i}{q_t}$ represents y, $\frac{t_i}{q_e}$ represents c, $\frac{1}{k_2}$ represent m, $\frac{1}{q_e^2}$ represent x. From the graph in Figure 7, we can obtain the parameter of PSO for the adsorption.

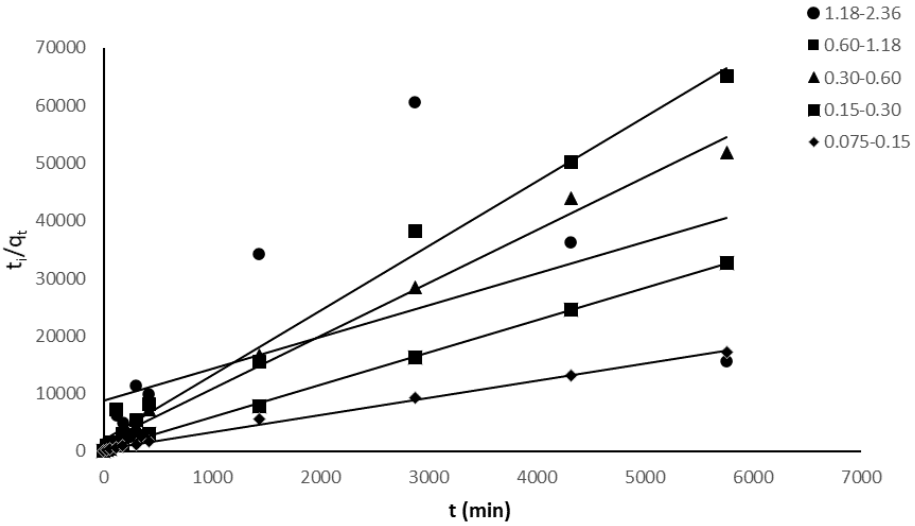

Figure 7. t_i/q_t with t (min) for every particle size.

Table 5. The kinetic parameter of the PSO model.

Sample	Particle Size (mm)	q_e (theo)	k_2 (g mg^{-1} min^{-1})	R^2	Fe	q_e (exp) (mg g^{-1})
Synthetic solution	1.18–2.36	0.4051	0.0005	0.1847	0.328	0.3675
	0.60–1.18	0.0894	0.0626	0.9903	0.046	0.086
	0.30–0.60	0.1086	0.054	0.9925	0.052	0.101
	0.15–0.30	0.1783	0.1094	0.9991	0.056	0.177
	0.075–0.15	0.3353	0.0241	0.9965	0.109	0.3085

From the obtained kinetic parameter of PFO and PSO in Table 4 and Table 5, the coefficient correlation of PSO is higher than PFO. Therefore, this study verified that the PSO model is more suitable for describing phosphate's kinetic adsorption onto raw MCS than the PFO model due to the lower value of Fe and the higher value of R^2 obtained [12].

In the PSO model, the kinetics of adsorption in this study is very slow because it needs a long contact period between adsorbent and adsorbate to reach equilibrium since the adsorption requires at least 2880 mins to reach equilibrium. The PSO model proves that the adsorbent, raw MCS have many active sites [34].

3.6. Isotherm model.

The adsorption isotherm mechanism in this study is done by plotting the Freundlich and Langmuir models (Figure 8) [32].

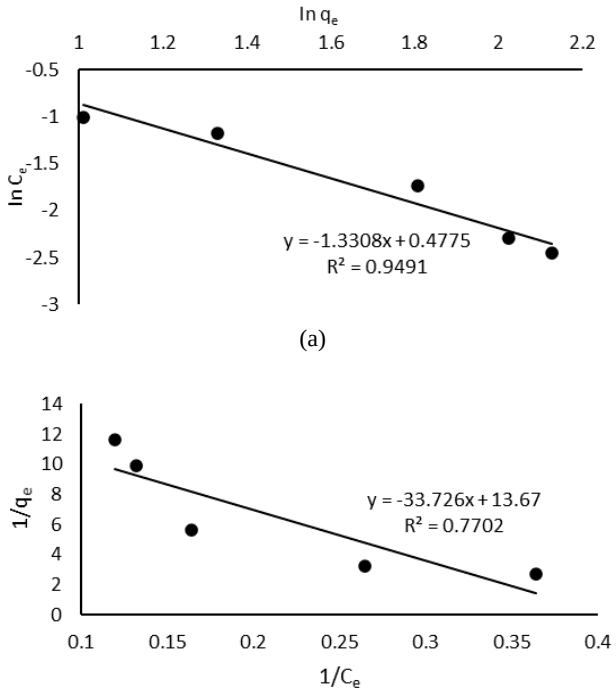

Figure 8. Experimental data of phoshate onto MCS fitted to (a) Freundlich model (b) Langmuir model.

Table 6. Parameter of isotherm model for the adsorption of phosphate on raw MCS

Isotherm model	*Parameter*	*Values*
Freundlich	n	−0.7514
	K_F (mg g^{-1})	1.612
	R^2	0.9491
Langmuir	q_{max} (mg g^{-1})	0.07315
	K_L (L mg^{-1})	−0.4049
	R^2	0.7702

The parameters obtained in Table 6 show that the Freundlich model had a higher correlation coefficient than the Langmuir model. It concluded that the adsorption process is heterogeneous and multilayer sorption [35].

4. Conclusions

The phosphate in the wastewater can damage the ecosystem and human health problems since phosphate in wastewater can contribute to eutrophication. Furthermore, the wasted MCS can lead to pollution due to the exposure because the MCS is hard to decompose naturally. This study successfully investigated phosphate's removal efficiency onto raw MCS and obtained the highest removal efficiency at 73% using 1.18 mm–2.36 mm particle size. The data fitted the PFO and PSO models. The highest correlation coefficient (R^2 = 0.9965) and lowest Fe value

which Fe = 0.086. The adsorption isotherm data well fitted the Freundlich model (R^2 =0.9491), signifying that the adsorption of phosphate onto raw MCS from synthetic wastewater occurred on the heterogeneous surface, and it is multilayer sorption. The physicochemical investigation of MCS showed a higher Ca content, which is 28%. A higher positive charged Ca content can increase phosphate adsorption, which is negatively charged. The findings showed that the MCS is a potential adsorbent to reduce phosphate in wastewater. Removing phosphate from domestic wastewater can be an alternative wastewater treatment in tertiary treatment.

Funding

This research was supported by the Ministry of Higher Education (MOHE) through Fundamental Research Grant Scheme (FRGS/1/2020/TK0/UTHM/02/22) or Vot No. K308.

Acknowledgments

The authors would like to thank Neo Environment Technology (NET), Centre for Diploma Studies (CeDS), Research Management Centre, Universiti Tun Hussein Onn Malaysia for their support.

Conflicts of Interest

The authors declare no conflict of interest.

References

1. Radini, S.; Marinelli, E.; Akyol, Ç.; Eusebi, A.L.; Vasilaki, V.; Mancini, A.; Frontoni, E.; Bischetti, G.B.; Gandolfi, C.; Katsou, E.; et al. Urban water-energy-food-climate nexus in integrated wastewater and reuse systems: Cyber-physical framework and innovations. *Applied Energy* **2021**, *298*, https://doi.org/10.1016/j.apenergy.2021.117268.
2. Chan-Pacheco, C.R.; Valenzuela, E.I.; Cervantes, F.J.; Quijano, G. Novel biotechnologies for nitrogen removal and their coupling with gas emissions abatement in wastewater treatment facilities. *Science of The Total Environment* **2021**, *797*, https://doi.org/10.1016/j.scitotenv.2021.149228.
3. Tsatsaros, J.H.; Bohnet, I.C.; Brodie, J.E.; Valentine, P. A transdisciplinary approach supports community-led water quality monitoring in river basins adjacent to the Great Barrier Reef, Australia. *Marine Pollution Bulletin* **2021**, *170*, https://doi.org/10.1016/j.marpolbul.2021.112629.
4. Huang, J.; Wang, C.; Qi, L.; Zhang, X.; Tang, G.; Li, L.; Guo, J.; Jia, Y.; Dou, X.; Lu, M. Phosphorus is more effective than nitrogen in restoring plant communities of heavy metals polluted soils. *Environmental Pollution* **2020**, *266*, https://doi.org/10.1016/j.envpol.2020.115259.
5. Chen, Q.; Ni, Z.; Wang, S.; Guo, Y.; Liu, S. Climate change and human activities reduced the burial efficiency of nitrogen and phosphorus in sediment from Dianchi Lake, China. *Journal of Cleaner Production* **2020**, *274*, https://doi.org/10.1016/j.jclepro.2020.122839.
6. Wu, H.; Wang, J.; Chen, J.; Wang, X.; Li, D.; Hou, J.; He, X. Advanced nitrogen and phosphorus removal by combining endogenous denitrification and denitrifying dephosphatation in constructed wetlands. *Journal of Environmental Management* **2021**, *294*, https://doi.org/10.1016/j.jenvman.2021.112967.
7. Arun, J.; Gopinath, K.P.; Vigneshwar, S.S.; Swetha, A. Sustainable and eco-friendly approach for phosphorus recovery from wastewater by hydrothermally carbonized microalgae: Study on spent bio-char as fertilizer. *Journal of Water Process Engineering* **2020**, *38*, https://doi.org/10.1016/j.jwpe.2020.101567.
8. de Almeida, M.L.S.; Lima, A.C.P.; Nagahama, K.d.J.; Santos, T.S.M. Application of the Southwell Plot method to determine equilibrium time in phosphate adsorption. *Journal of Contaminant Hydrology* **2021**, *242*, https://doi.org/10.1016/j.jconhyd.2021.103841.
9. Martins, M.C.; Santos, E.B.H.; Marques, C.R. First study on oyster-shell-based phosphorous removal in saltwater — A proxy to effluent bioremediation of marine aquaculture. *Science of The Total Environment* **2017**, *574*, 605-615, https://doi.org/10.1016/j.scitotenv.2016.09.103.
10. Paradelo, R.; Conde-Cid, M.; Cutillas-Barreiro, L.; Arias-Estévez, M.; Nóvoa-Muñoz, J.C.; Álvarez-Rodríguez, E.; Fernández-Sanjurjo, M.J.; Núñez-Delgado, A. Phosphorus removal from wastewater using mussel shell: Investigation on retention mechanisms. *Ecological Engineering* **2016,** *97*, 558-566, https://doi.org/10.1016/j.ecoleng.2016.10.066.

11. Lili, J.; Wendong, S.; Danyi, W.; Dongjiao, J.; Lu, C.; Yaning, W.; Jian, G.; Hailong, Z. Modified mussel shell powder for microalgae immobilization to remove N and P from eutrophic wastewater. *Bioresource Technology* **2019,** *284*, 36-42, https://doi.org/10.1016/j.biortech.2019.03.112.
12. Salim, N.A.A.; Fulazzaky, M.A.; Puteh, M.H.; Khamidun, M.H.; Yusoff, A.R.M.; Abdullah, N.H.; Nuid, M. Adsorption of phosphate from aqueous solution onto iron-coated waste mussel shell: Physicochemical characteristics, kinetic, and isotherm studies. *Biointerface Research in Applied Chemistry* **2021,** *11*, 12831-12842, https://doi.org/10.33263/BRIAC115.1283112842.
13. Denil, D.; Ching, F. F.; Ransangan, J. Health Risk Assessment Due to Heavy Metals Exposure via Consumption of Bivalves Harvested from Marudu Bay. *MalaysiaOpen Journal of Marine Science* **2017,** *7*, 494-510, https://doi.org/10.4236/ojms.2017.74035.
14. Köse, T.E.; Kıvanç, B. Adsorption of phosphate from aqueous solutions using calcined waste eggshell. *Chemical Engineering Journal* **2011,** *178*, 34-39, https://doi.org/10.1016/j.cej.2011.09.129.
15. Evangelia, P.; Nasia, K.; Loukas, K.; Panayiotis, K.; Petros, N.; Georgios, C.; Ioannis, V. Turning calcined waste egg shells and wastewater to Brushite: Phosphorus adsorption from aqua media and anaerobic sludge leach water. *Journal of Cleaner Production* **2018,** *178*, 419-428, https://doi.org/10.1016/j.jclepro.2018.01.014.
16. DR6000 Laboratory Spectrophotometer. Available online: https://www.hach.com (accessed on 28 July **2021**).
17. Asami, H.; Golabi, M.; Albaji, M. Simulation of the biochemical and chemical oxygen demand and total suspended solids in wastewater treatment plants: Data-mining approach. *Journal of Cleaner Production* **2021,** *296*, https://doi.org/10.1016/j.jclepro.2021.126533.
18. Salim, N.; Abdullah, N. H.; Muhammad, K.; Arman, M.; Khamidun, M. H.; Fulazzaky, M.A.; Mohd Yusoff, A.R.; Othman, M.H.; Puteh, M.H. Adsorption of phosphate from aqueous solutions using waste mussel shell. *MATEC Web of Conferences* **2018,** *250*, https://doi.org/10.1051/matecconf/201825006013.
19. Gong, C.; Qionghui, L.; Zhan, S.; Sheng, S.; Jie, F. Preparation, optimization, and application of sustainable ceramsite substrate from coal fly ash/waterworks sludge/oyster shell for phosphorus immobilization in constructed wetlands. *Journal of Cleaner Production* **2018,** *175*, 572-581, https://doi.org/10.1016/j.jclepro.2017.12.102.
20. Irwin, M.; Fumitake, T. Cyanide removal study by raw and iron-modified synthetic zeolites in batch adsorption experiments. *Journal of Water Process Engineering* **2018,** *22*, 80-86, https://doi.org/10.1016/j.jwpe.2018.01.013.
21. Nimibofa, A.; Augustus, N.E.; Donbebe, W. Modelling and Interpretation of Adsorption Isotherms. *Journal of Chemistry* **2017,** *2017*, https://doi.org/10.1155/2017/3039817.
22. Chang, J.; Shen, Z.; Hu, X.; Emily, S.; Chunyue, C.; Qingjie, G.; Tian, H. Adsorption of Tetracycline by Shrimp Shell Waste from Aqueous Solutions: Adsorption Isotherm, Kinetics Modeling, and Mechanism. *ACS Omega* **2020,** *5*, 3467−3477, https://doi.org/10.1021/acsomega.9b03781.
23. Nandiyanto, A.; Oktiani, R.; Ragadhita, R. How to Read and Interpret FTIR Spectroscope of Organic Material. *Indonesian Journal of Science and Technology* **2019,** *4*, 97-118, https://doi.org/10.17509/ijost.v4i1.15806.
24. Bratu, I.; Grecu, R.; Constantinescu, R.; Iliescu, T. Molecular relaxation processes of 2-bromopropane in solutions from IR ν(C–Br) band shape analysis1The paper was presented in part at the XXIX CSI. Spectrochimica Acta Part A. *Molecular and Biomolecular Spectroscopy* **1998,** *54*, 1386-1425, https://doi.org/10.1016/S1386-1425(97)00252-7.
25. Mat Lazim, Z.; Salmiati; Hadibarata, T.; Yusop, Z.; Nazifa, T.H.; Abdullah, N.H.; Nuid, M.; Abdul Salim, N.A.; Zainuddin, N.A.; Ahmad, N. Bisphenol a removal by adsorption using waste biomass: Isotherm an kinetic studies. *Biointerface Research in App. Chemistry* **2021,** *11*, 8467-8481, https://doi.org/10.33263/BRIAC111.84678481.
26. Kashif, I.; Hamad, K.; Aqif, A.C. Zinc-substituted hydroxyapatite. Handbook of Ionic Substituted Hydroxyapatites. In: *Woodhead Publishing Series in Biomaterials*. Khan, A.S.; Chaudhry, A.A. Woodhead Publishing, **2020**; pp. 217-236, https://doi.org/10.1016/B978-0-08-102834-6.00009-4.
27. Kim, Y.; Kim, D.; Kang, S.; Ham, Y.; Choi, J.H.; Hong, Y.; Ryoo, K. Use of Powdered Cockle Shell as a Bio-Sorbent Material for Phosphate Removal from Water. *Bulletin of the Korean Chemical Society* **2018**, *39*, 1362-1367, https://doi.org/10.1002/bkcs.11606.
28. Torit, J.; Phihusut, D. Phosphorus removal from wastewater using eggshell ash. *Environ Science Pollution Research* **2019,** *26*, 34101–34109, https://doi.org/10.1007/s11356-018-3305-3.
29. Kasim, N.Z.; Abd Malek, N.A.A.; Hairul Anuwar, N.S.; Hamid, N.H. Adsorptive removal of phosphate from aqueous solution using waste chicken bone and waste cockle shell. *Materials Today: Proceedings* **2021,** *31*, A1-A5, https://doi.org/10.1016/j.matpr.2020.09.687.
30. Abdul Salim, N.A.; Fulazzaky, M.A.; Ahmad Zaini, M.A.; Puteh, M.H.; Khamidun, M.H.; Mohd Yusoff, A.R.; Abdullah, N.H.; Ahmad, N.; Mat Lazim, Z.; Nuid, M. Phosphate removal from wastewater in batch system using waste mussel shell. *Biointerface Research in Applied Chemistry* **2021,** *11*, 11473-11486, https://doi.org/10.33263/BRIAC114.1147311486.

31. Pierce, R.; Stacey, K.; Bardini, C. Linear functions: Teaching strategies and 'students' conceptions associated with y = mx + c. *Pedagogies: An International Journal* **2010,** *5,* 202-215, https://doi.org/10.1080/1554480X.2010.486151.
32. Abdul Salim, N.A.; Fulazzaky, M.A.; Puteh, M.H.; Khamidun, M.H.; Mohd Yusoff, A.R.; Abdullah, N.H.; Ahmad, N.; Mat Lazim, Z.; Nuid, M. Adsorption of Phosphate from Aqueous Solution onto Iron-coated Waste Mussel Shell: Physicochemical Characteristics, Kinetic and Isotherm Studie. *Biointerface Research in Applied Chemistry* **2021,** *11,* 12831-12842, https://doi.org/10.33263/BRIAC115.1283112842.
33. Jianlong, W.; Xuan, G. Adsorption kinetic models: Physical meanings, applications, and solving methods. *Journal of Hazardous Materials* **2020,** *390,* https://doi.org/10.1016/j.jhazmat.2020.122156.
34. Jianlong, W.; Xuan, G. Adsorption isotherm models: Classification, physical meaning, application and solving method. *Chemosphere* **2020,** *258,* https://doi.org/10.1016/j.chemosphere.2020.127279.
35. Hasan, A. Production of low-cost adsorbent with small particle size from calcium carbonate rich residue carbonatation cake and their high performance phosphate adsorption applications. *Journal of Materials Research and Technology* **2021,** *11,* 428-447, https://doi.org/10.1016/j.jmrt.2021.01.054.